Med Biol Eng Comput (2017) 55:1743–1761
DOI 10.1007/s11517-017-1613-2

ORIGINAL ARTICLE

Epileptic seizure classifications of single-channel scalp EEG data using wavelet-based features and SVM

Suparerk Janjarasjitt[1]

Received: 15 April 2016 / Accepted: 25 January 2017 / Published online: 13 February 2017
© International Federation for Medical and Biological Engineering 2017

Abstract In this study, wavelet-based features of single-channel scalp EEGs recorded from subjects with intractable seizure are examined for epileptic seizure classification. The wavelet-based features extracted from scalp EEGs are simply based on detail and approximation coefficients obtained from the discrete wavelet transform. Support vector machine (SVM), one of the most commonly used classifiers, is applied to classify vectors of wavelet-based features of scalp EEGs into either seizure or non-seizure class. In patient-based epileptic seizure classification, a training data set used to train SVM classifiers is composed of wavelet-based features of scalp EEGs corresponding to the first epileptic seizure event. Overall, the excellent performance on patient-dependent epileptic seizure classification is obtained with the average accuracy, sensitivity, and specificity of, respectively, 0.9687, 0.7299, and 0.9813. The vector composed of two wavelet-based features of scalp EEGs provide the best performance on patient-dependent epileptic seizure classification in most cases, i.e., 19 cases out of 24. The wavelet-based features corresponding to the 32–64, 8–16, and 4–8 Hz subbands of scalp EEGs are the mostly used features providing the best performance on patient-dependent classification. Furthermore, the performance on both patient-dependent and patient-independent epileptic seizure classifications are also validated using tenfold cross-validation. From the patient-independent epileptic seizure classification validated using tenfold cross-validation, it is shown that the best classification performance is achieved using the wavelet-based features corresponding to the 64–128 and 4–8 Hz subbands of scalp EEGs.

Keywords Electroencephalogram · Seizure · Support vector machine · Classification · Wavelet transform

1 Introduction

Indeed, machine learning plays a crucial role in a variety of fields and has been widely applied. Ones of the key research fields are biology and medicine. Computational techniques and tools derived from machine learning concepts and theories have been applied to obtain better diagnosis and prognosis of diseases, treatments, and also health monitoring systems. Epilepsy, one of the most common neurological disorders, has been a challenging subject and gained a great attention from researchers. Epilepsy is characterized by recurrent seizures that are physical reactions to sudden, usually brief, excessive electrical discharges in clusters of nerve cells [21]. Approximately 50 million people worldwide have epilepsy, and most of the people with epilepsy live in low- and middle-income countries [21].

An electroencephalogram (EEG) that is recorded using electrodes placed on the scalp is the most common diagnosis test for epilepsy [13]. The EEG that quantifies electrical activity of the brain provides ability to detect abnormalities in the brain. Epileptic seizure classification and detection are a crucial task of epilepsy diagnosis where specific features and patterns of the EEG such as monomorphic waveforms, polymorphic waveforms, spike and sharp wave complexes, or periods of reduced electrocerebral activity [8, 17, 20] are needed to be identified and detected. The scalp EEG is very sensitive to signal attenuation and artifacts, and also has poor spatial resolution. An intracranial EEG

✉ Suparerk Janjarasjitt
suparerk.j@ubu.ac.th

[1] Department of Electrical and Electronic Engineering, Ubon Ratchathani University, 85 Sathonlamak Road, Warin Chamrap, Ubon Ratchathani 34190, Thailand

or an electrocorticogram (ECoG) is an alternative approach to detect the electrical activity of the brain by placing electrodes on the cortex. The intracranial EEG therefore provides a better characteristic of brain activity; however, it is a more complicated and expensive diagnostic test. Previously most of studies on epileptic seizure classification and detection examine intracranial EEG data.

A number of quantitative features extracting from either scalp EEG or intracranial EEG including time-domain features, frequency-domain or transform-domain features, and also nonlinear features have been applied and shown to be useful for epileptic seizure classification and detection. Several of those quantitative features have been applied to both scalp and intracranial EEGs for epileptic seizure classification and detection. Some common time-domain features [4, 9, 14, 18] are Hjorth parameters, zero crossing, root mean square (RMS), line length, number of local maxima and minima, and various statistical values such as variance. Average power, total power, powers of spectral subbands, peak frequency, mean frequency, and median frequency are common frequency-domain features that are typically obtained from the discrete Fourier transform, power spectral density (PSD), and the discrete wavelet transform [9, 12, 15]. In particular, the time-domain features of single-channel EEGs that provide the best epileptic seizure classification [9] with respect to the area under receiver operating characteristic (ROC) curve are line length, nonlinear energy, variance, power, and maximum. Recently, several nonlinear quantitative measures [6, 7, 14] such as Shannon entropy, approximate entropy, fractal dimension, maximum Lyapunov exponent, and spectral exponent are common nonlinear features applied for epileptic seizure classification and detection.

Various computational techniques and classifiers have been used to classify EEG into corresponding physiological and pathological states associated with epilepsy such as ictal state (EEG associated with an epileptic seizure event), interictal, pre-ictal, and post-ictal states. Machine learning methods are a popular choice recently applied for classifying a set of multiple quantitative features of EEG. Support vector machine (SVM) classifiers are applied to scalp EEG data [12, 16–18]. However, in [4], a linear discriminant classifier is applied for neonatal seizure detection. Evolutionary neural networks are also applied for epileptic seizure classification [7]. Epileptic seizure classification and detection can be performed using either patient-independent- or patient-dependent-based algorithms. A wide range of success on epileptic seizure classification and detection has been reported. In general, patient-dependent-based algorithms provide better performance on epileptic seizure classification. Also, the performance on epileptic seizure classification and detection depends on seizure morphologies [12].

In particular, for epileptic seizure classification and detection using scalp EEGs, sixty-five quantitative features of multichannel scalp EEGs were examined and utilized in Ref. [9]. All sixty-five quantitative features including features derived from time-domain analyses, the discrete wavelet transform, the continuous wavelet transform, and discrete Fourier transform have been previously applied in various studies. It was shown that there is a performance trade-off between the sensitivity and the specificity. The best performance on seizure classification is achieved using the relative power obtained from the discrete wavelet transform corresponding to a 12.5–25 Hz subband with the sensitivity of 71.32% and the specificity of 79.67% when the optimal threshold is used [9]. On the other hand, averaged and integrated powers of multichannel bipolar EEGs focusing on the 2.5–12 Hz subband were applied for epileptic seizure detection in Ref. [5]. The sensitivity of epileptic seizure detection was 87.3% for subjects with temporal lobe epilepsy (TLE) and extra-temporal lobe epilepsy (ETLE).

The energies determined from the coefficients of discrete wavelet transform corresponding to four subbands of multiple-channel scalp EEGs are used for patient-dependent epileptic seizure detection in Ref. [17]. Overall, 131 of 139 epileptic seizure events are detected for the patient-dependent epileptic seizure detection while there are 15 false detections [17]. In Ref. [12], seven quantitative features of 19-channel scalp EEGs including subband powers obtained from the continuous wavelet transform and various time-domain features and an SVM classifier were applied for epileptic seizure detection where the prior knowledge on diversity of seizure morphologies was taken into account. The high correct detection rate (between 85 and 100%) and low false alarm rates (between 0.2 and 0.4 per hour) were achieved [12]. A large set of quantitative features of scalp EEGs were applied in Ref. [7] for patient-dependent epileptic seizure classification. The main features examined belonged to morphological-based features, time-domain features, frequency-domain, features, and a nonlinear feature. The average sensitivity and specificity obtained were 89.01 and 94.71%, respectively.

In this study, performances on epileptic seizure classification using wavelet-based features are examined by, in particular, focusing on patient-dependent classification. The number of channels of scalp EEGs is minimized which yields a small number of wavelet-based features applied to epileptic seizure classification. The wavelet-based features denoted by λ_l are given by the logarithm to base 2 of variance of detail and approximation coefficients of scalp EEGs. Such wavelet-based features are computationally relevant to the power spectral density (PSD) [1]. The wavelet-based approach, however, allows an unbiased estimate [1]. SVM is used as a binary classifier to discriminate scalp

EEG epochs associated with epileptic seizure event from scalp EEG epochs associated with pre-ictal and post-ictal states, i.e., non-seizure period. The patient-dependent epileptic seizure classification using wavelet-based features is evaluated using two schemes. First, the wavelet-based features of scalp EEG epochs corresponding to the first epileptic seizure event are used as a training data. This approach complies with the actual application when it is applied to real-time or online epileptic seizure classification and detection. Furthermore, k-fold cross-validation is applied to the patient-dependent epileptic seizure classification using wavelet-based features in the second scheme. The performance on patient-independent epileptic seizure classification is also evaluated using k-fold cross-validation.

2 Materials and methods

2.1 Data and subjects

Scalp EEG data of subjects with intractable seizures examined in this study were obtained from the CHB-MIT Scalp EEG Database (available online at http://www.physionet.org/pn6/chbmit/). The database was collected at the Children's Hospital Boston [3]. All subjects were monitored for up to several days following withdrawal of anti-seizure medication in order to characterize their seizures and assess their candidacy for surgical intervention [3]. All protected health information (PHI) in the original recordings was replaced with surrogate information in order to protect the privacy of the subjects [3]. The scalp EEG recordings were acquired using a sampling rate of 256 Hz with 16 bit resolution [3]. The international 10–20 system of EEG electrode positions and nomenclature was used for the recordings [3].

There are 24 cases of scalp EEG recordings, referred to as chb01, chb02, chb03, and so on. The first 23 cases, excluding the chb24 case, were recorded from 22 subjects (5 males, ages 3–22 years old, and 17 females, ages 1.5–19 years old) [3]. The chb01 and chb21 cases were obtained from the same subject. There are a total of 198 epileptic seizure events. Further details on scalp EEG data and cases can be obtained at http://www.physionet.org/pn6/chbmit/.

2.2 Wavelet-based features of scalp EEGs

The discrete wavelet transform is a representation of a signal using a countably infinite set of wavelets that constitutes an orthonormal basis [11]. The wavelet transform can be interpreted as a generalized filter bank [22] as the so-called mother wavelet is typically associated with a bandpass filter. Also, the wavelet transform can be interpreted in the context of multiresolution analysis (MRA) [10]. The multiresolution analysis generally consists of a sequence of successive approximation spaces [19]. Furthermore, the multiresolution analysis leads to a hierarchical scheme for the computation of the wavelet coefficients of a given function [19].

A signal $x[n]$ is decomposed into approximations and details using the scaling and wavelet functions that, respectively, correspond to lowpass halfband filter and highpass halfband filter. This can be expressed as

$$x[n] = \sum_k a_0[k]\phi_{0,k}[n] \tag{1}$$

$$= \sum_k a_1[k]\phi_{1,k}[n] + \sum_k d_1[k]\psi_{1,k}[n] \tag{2}$$

where the scaling function $\phi_{1,k}[n]$ and the wavelet function $\psi_{1,k}[n]$ are, respectively, an orthonormal basis for the space V_1 and the orthogonal complement of V_1, denoted by W_1, and the space $V_0 = V_1 \oplus W_1$. The approximation coefficients $a_1[n]$ and the detail coefficients $d_1[n]$ can be obtained by

$$a_1[n] = \sum_k a_0[k]h[k-2n] \tag{3}$$

$$d_1[n] = \sum_k a_0[k]g[k-2n] \tag{4}$$

where $h[n]$ and $g[n]$ are, respectively, the impulse response of lowpass halfband filter and highpass halfband filter.

For a single-level discrete wavelet decomposition at level l, the approximation coefficients $a_l[n]$ can be obtained by convolving the approximation coefficients $a_{l-1}[n]$ with the time-reversed filter of $h[n]$, i.e., $\tilde{h}[n]$, followed by the downsampling and, similarly, the detail coefficients $d_l[n]$ can be obtained by convolving the approximation coefficients $a_{l-1}[n]$ with the time-reversed filter of $g[n]$, i.e., $\tilde{g}[n]$, followed by the downsampling.

From the L-level discrete wavelet decomposition, there are L detail coefficients, i.e., $d_1, d_2, \cdots, d_L$, and one approximation coefficients, i.e., a_L, obtained. Wavelet-based features proposed for epileptic seizure classification in this study are determined by taking the logarithm to base 2 of variance of detail coefficients and approximation coefficients. The wavelet-based features obtained from the detail coefficients d_l are denoted by λ_l, and the wavelet-based feature obtained from the approximation coefficients a_L is denoted by λ_{L+1}. Therefore, the wavelet-based features are given by

$$\lambda_l = \log_2(\mathrm{var}(d_l)), \quad \text{where } l = 1, 2, \ldots, L \text{ and} \tag{5}$$

$$\lambda_{L+1} = \log_2(\mathrm{var}(a_L)) \tag{6}$$

2.3 Data analysis and classification

Segments of single-channel scalp EEGs around epileptic seizure events (12 min before seizure onset and 12 min after seizure offset, unless limited by the beginning, the end of recording, or the contiguous epileptic seizure events) are used in this study. The scalp EEG segments are divided into epochs with length of 512 samples (2 s) and with 50% overlap. Such short length of scalp EEG epochs is chosen to be able to capture characteristics of a brief lapse of epileptic seizure event. Scalp EEG epochs associated with epileptic seizure event are categorized as an SZ class while scalp EEG epochs associated with pre-ictal and post-ictal states are categorized as an NS class. The number of SZ and NS epochs for each case is summarized in Table 1.

The second-order Daubechies wavelets are used for the discrete wavelet decomposition. The Daubechies wavelet family, one of the most commonly used wavelet families, has several nice characteristics including orthogonality and finite compact support. Higher-order Daubechies wavelets corresponds to higher regularity and also a number of vanishing moments. Scalp EEG epochs are decomposed into 7 levels that are the maximum level of wavelet decomposition using the second-order Daubechies. Accordingly, seven detail coefficients, i.e., d_1, d_2, d_3, d_4, d_5, d_6 and d_7, and one approximation coefficients, i.e., a_7, are obtained. The coefficients d_1, d_2, d_3, d_4, d_5, d_6, d_7, and a_7 correspond approximately to 64–128, 32–64, 16–32, 8–16, 4–8, 2–4, 1–2, and 0–1 Hz subbands, respectively.

A feature vector applied for epileptic seizure classification is composed of all combinations of wavelet-based features of scalp EEG epochs, ranging from two wavelet-based features, i.e., (λ_i, λ_j) where $i \neq j$, to seven wavelet-based features, i.e., $(\lambda_i, \lambda_j, ..., \lambda_n, \lambda_o)$ where $i \neq j \neq k \neq l \neq m \neq n \neq o$. Feature vectors of scalp EEG epochs are classified using support vector machine (SVM). The radial basis function (RBF) kernel is used to train an SVM classifier. Scalp EEG epochs of both SZ and NS classes obtained from the first seizure event of each subject are used as training data sets. The classification and the performance evaluation are performed by a case-by-case basis, i.e., patient-dependent epileptic

Table 1 Details of scalp EEG epochs

Case	Seizure duration (s)			No. of epochs			
				All seizures		The first seizure	
	Max	Min	Mean	SZ	NS	SZ	NS
chb01	101	27	63.1	428	9147	38	1281
chb02	82	9	57.3	166	3049	79	1264
chb03	69	47	57.4	388	9406	50	1078
chb04	116	49	94.5	370	5744	47	1436
chb05	120	96	111.6	548	6877	113	1133
chb06	20	12	15.3	133	13,151	13	1436
chb07	143	86	108.3	319	3795	84	1436
chb08	264	134	183.8	909	6774	169	1436
chb09	79	62	69.0	268	5364	62	1436
chb10	89	35	63.9	433	9587	33	1436
chb11	752	22	268.7	800	3820	20	1014
chb12	97	13	36.9	1395	25,773	59	1438
chb13	70	17	44.6	511	13,520	42	1436
chb14	41	14	21.1	153	11,099	12	1436
chb15	205	31	99.6	1952	22,497	123	988
chb16	14	6	8.4	64	11,441	7	1436
chb17	115	88	97.7	287	3730	88	1436
chb18	68	30	54.5	315	6924	48	790
chb19	81	77	78.7	230	3102	76	1015
chb20	49	29	36.8	278	10,360	27	810
chb21	81	12	49.8	191	5338	54	1436
chb22	74	58	68.0	198	3432	56	892
chb23	113	20	60.6	410	9269	111	1436
chb24	70	16	31.9	479	16735	23	1436

Table 2 Statistical values (Mean±SD) of wavelet-based features of scalp EEG epochs

Case	Class	Feature							
		λ_1	λ_2	λ_3	λ_4	λ_5	λ_6	λ_7	λ_8
chb01	SZ	7.64 ± 1.4	9.54 ± 0.8	11.29 ± 0.6	13.96 ± 0.8	16.58 ± 1.3	17.87 ± 1.8	17.96 ± 1.8	19.03 ± 1.9
	NS	4.56 ± 1.2	8.40 ± 1.1	9.69 ± 1.0	9.96 ± 0.9	11.95 ± 1.1	13.03 ± 1.4	13.59 ± 1.8	14.61 ± 2.0
chb02	SZ	8.08 ± 1.5	10.93 ± 1.3	13.23 ± 1.2	15.20 ± 1.0	16.69 ± 1.2	17.17 ± 1.6	16.91 ± 1.9	17.74 ± 2.0
	NS	7.47 ± 4.7	8.39 ± 4.0	9.18 ± 2.7	10.81 ± 2.0	12.38 ± 1.7	13.92 ± 1.8	14.90 ± 2.0	16.13 ± 2.1
chb03	SZ	9.85 ± 1.4	11.44 ± 1.5	12.38 ± 1.2	12.91 ± 0.9	15.05 ± 0.8	16.12 ± 1.1	16.80 ± 1.8	17.75 ± 1.9
	NS	5.66 ± 1.8	7.48 ± 2.1	8.58 ± 2.0	8.82 ± 1.5	9.89 ± 1.6	11.61 ± 2.1	12.72 ± 2.4	13.71 ± 6.6
chb04	SZ	9.03 ± 2.7	9.97 ± 2.2	11.00 ± 1.7	11.50 ± 0.7	13.47 ± 0.6	14.97 ± 1.1	15.10 ± 1.5	15.34 ± 1.9
	NS	6.69 ± 5.9	8.27 ± 5.4	9.30 ± 4.2	10.26 ± 3.4	11.27 ± 2.7	12.45 ± 2.7	13.28 ± 2.8	15.17 ± 3.5
chb05	SZ	8.84 ± 1.0	11.54 ± 0.8	13.57 ± 1.1	15.22 ± 1.5	17.16 ± 1.4	18.36 ± 1.7	18.06 ± 2.1	18.48 ± 2.0
	NS	4.41 ± 2.0	6.05 ± 2.1	8.25 ± 1.6	10.91 ± 0.9	13.57 ± 1.0	14.66 ± 1.2	14.92 ± 1.6	15.90 ± 1.9
chb06	SZ	8.74 ± 1.6	10.23 ± 1.1	11.26 ± 0.7	12.19 ± 0.5	13.40 ± 1.5	14.96 ± 1.5	14.96 ± 1.4	16.87 ± 1.4
	NS	7.36 ± 1.3	10.40 ± 1.3	12.28 ± 1.0	13.50 ± 0.8	15.16 ± 1.0	16.15 ± 1.0	16.34 ± 1.4	17.29 ± 1.7
chb07	SZ	10.27 ± 2.0	11.88 ± 1.9	13.30 ± 1.5	14.67 ± 0.9	16.51 ± 0.8	18.23 ± 1.4	18.49 ± 1.6	18.66 ± 1.8
	NS	5.93 ± 1.8	7.72 ± 1.6	9.21 ± 1.4	10.94 ± 1.8	13.08 ± 2.6	14.69 ± 3.2	15.37 ± 3.3	16.12 ± 3.0
chb08	SZ	2.18 ± 1.3	5.44 ± 1.5	8.41 ± 1.5	12.00 ± 1.4	15.42 ± 1.5	17.83 ± 1.8	17.88 ± 2.1	18.90 ± 2.0
	NS	1.52 ± 1.1	4.77 ± 1.0	7.17 ± 0.7	9.76 ± 0.9	12.29 ± 1.1	13.89 ± 1.4	14.47 ± 1.6	15.57 ± 1.8
chb09	SZ	7.25 ± 1.5	10.83 ± 1.5	14.30 ± 1.7	16.87 ± 2.0	18.13 ± 1.6	17.95 ± 1.5	18.18 ± 1.6	19.65 ± 2.1
	NS	2.85 ± 2.3	5.85 ± 1.6	8.69 ± 1.4	11.19 ± 1.0	13.19 ± 1.1	13.92 ± 2.0	14.69 ± 2.6	15.73 ± 2.4
chb10	SZ	6.03 ± 0.4	10.00 ± 0.5	13.41 ± 0.7	16.33 ± 0.7	18.20 ± 0.7	17.93 ± 0.9	17.69 ± 1.1	18.39 ± 2.1
	NS	4.76 ± 1.7	7.01 ± 1.6	8.90 ± 1.1	11.53 ± 0.7	14.85 ± 0.9	17.22 ± 0.9	17.73 ± 1.3	18.32 ± 1.5
chb11	SZ	8.14 ± 2.2	9.50 ± 1.6	11.81 ± 1.0	13.91 ± 0.7	16.05 ± 0.8	16.27 ± 1.2	16.78 ± 1.0	17.30 ± 1.4
	NS	5.68 ± 1.6	7.53 ± 1.3	8.99 ± 1.1	10.44 ± 0.9	12.28 ± 1.1	13.58 ± 1.4	14.50 ± 1.7	15.64 ± 1.8
chb12	SZ	3.19 ± 1.2	7.02 ± 1.4	9.82 ± 1.5	12.06 ± 1.1	14.39 ± 1.2	15.41 ± 2.0	15.55 ± 2.2	17.08 ± 2.3
	NS	2.46 ± 0.9	6.23 ± 0.9	8.85 ± 0.8	10.92 ± 1.1	13.03 ± 1.5	14.11 ± 1.5	14.82 ± 1.8	15.73 ± 3.6
chb13	SZ	2.60 ± 0.5	5.35 ± 0.5	8.17 ± 0.4	11.64 ± 0.6	14.26 ± 0.9	16.25 ± 1.0	16.19 ± 1.9	16.53 ± 1.7
	NS	3.57 ± 1.4	6.38 ± 1.4	8.92 ± 1.2	11.93 ± 1.1	14.03 ± 1.3	13.88 ± 1.4	14.28 ± 1.6	15.40 ± 1.8
chb14	SZ	2.79 ± 0.5	5.74 ± 0.4	7.51 ± 0.6	9.31 ± 1.1	11.04 ± 1.8	11.84 ± 3.3	12.91 ± 2.7	14.53 ± 3.0
	NS	1.75 ± 1.2	5.26 ± 0.9	8.46 ± 1.0	11.50 ± 1.1	14.15 ± 1.1	15.76 ± 1.2	16.07 ± 1.5	16.46 ± 1.6
chb15	SZ	2.26 ± 0.3	4.99 ± 0.4	8.01 ± 0.5	10.73 ± 0.7	12.67 ± 0.9	12.38 ± 1.0	11.84 ± 1.5	13.14 ± 2.0
	NS	2.24 ± 0.8	4.23 ± 0.8	6.14 ± 0.7	8.40 ± 0.8	9.65 ± 0.9	10.55 ± 1.0	10.90 ± 1.3	11.84 ± 1.8
chb16	SZ	5.83 ± 0.5	9.48 ± 0.6	12.16 ± 0.4	12.37 ± 0.4	12.77 ± 0.8	13.78 ± 0.9	14.59 ± 1.6	16.16 ± 1.7
	NS	3.83 ± 1.3	6.59 ± 1.1	8.32 ± 1.0	9.52 ± 1.0	11.63 ± 1.2	13.08 ± 1.6	13.88 ± 1.9	15.20 ± 2.1
chb17	SZ	3.21 ± 0.7	5.05 ± 0.8	7.16 ± 0.8	9.53 ± 0.9	11.88 ± 0.9	13.20 ± 1.1	12.67 ± 1.7	13.60 ± 1.8
	NS	1.70 ± 1.1	3.19 ± 0.6	4.50 ± 0.6	6.90 ± 0.7	9.50 ± 0.8	10.71 ± 1.2	11.20 ± 1.8	12.25 ± 2.0
chb18	SZ	5.26 ± 3.4	6.81 ± 2.6	8.23 ± 1.5	10.38 ± 0.9	13.21 ± 1.1	14.57 ± 1.0	14.88 ± 2.0	15.12 ± 2.7
	NS	-0.37 ± 2.0	2.14 ± 1.6	4.78 ± 1.3	7.29 ± 1.0	8.83 ± 1.1	9.23 ± 1.4	9.58 ± 1.9	10.69 ± 2.3
chb19	SZ	9.18 ± 3.1	10.71 ± 3.1	12.16 ± 3.0	13.48 ± 3.1	14.90 ± 3.6	15.13 ± 4.4	15.08 ± 4.6	16.82 ± 4.4
	NS	4.31 ± 2.7	6.24 ± 2.1	7.55 ± 1.8	9.06 ± 1.1	10.95 ± 1.2	12.64 ± 1.8	13.87 ± 2.3	15.01 ± 4.4
chb20	SZ	4.76 ± 1.0	7.41 ± 1.4	9.29 ± 1.9	10.92 ± 2.0	13.09 ± 2.1	14.97 ± 2.3	14.70 ± 1.9	15.88 ± 2.0
	NS	1.80 ± 0.4	4.95 ± 0.4	7.39 ± 0.5	9.63 ± 0.7	11.55 ± 0.9	12.61 ± 1.1	13.15 ± 1.4	14.04 ± 1.6
chb21	SZ	2.18 ± 0.6	5.55 ± 0.4	8.91 ± 0.5	11.78 ± 0.8	13.53 ± 0.9	14.09 ± 1.2	15.32 ± 1.3	16.08 ± 1.5
	NS	1.69 ± 0.6	4.69 ± 0.4	7.37 ± 0.4	9.93 ± 0.6	11.76 ± 0.7	12.61 ± 1.0	13.16 ± 1.4	14.23 ± 1.7
chb22	SZ	7.27 ± 2.0	8.90 ± 1.4	11.02 ± 0.6	13.66 ± 0.7	16.24 ± 0.9	17.31 ± 1.0	17.20 ± 1.5	17.68 ± 1.6
	NS	5.65 ± 2.0	7.50 ± 1.6	8.89 ± 1.3	10.00 ± 0.8	11.57 ± 1.0	12.68 ± 1.5	13.48 ± 1.9	14.96 ± 1.8
chb23	SZ	11.09 ± 1.5	12.49 ± 1.5	13.34 ± 1.3	13.02 ± 0.9	15.08 ± 1.0	17.42 ± 1.6	18.36 ± 1.6	18.75 ± 1.6
	NS	4.03 ± 3.2	6.63 ± 2.8	8.54 ± 2.0	9.83 ± 1.1	11.19 ± 1.1	12.32 ± 1.2	12.87 ± 1.6	14.04 ± 1.8
chb24	SZ	5.03 ± 2.1	8.15 ± 3.0	11.47 ± 2.9	14.68 ± 2.6	17.33 ± 3.0	19.65 ± 4.0	19.37 ± 3.8	19.58 ± 3.6
	NS	2.58 ± 0.2	4.53 ± 0.3	7.16 ± 0.3	9.74 ± 0.6	11.92 ± 0.7	13.19 ± 0.9	14.06 ± 1.3	14.91 ± 1.3

seizure classification. Furthermore, to validate a generalized performance of wavelet-based features on both patient-dependent and patient-independent epileptic seizure classifications, tenfold cross-validations are applied using feature vectors composing of two wavelet-based features, i.e., (λ_i, λ_j). For each case, the feature vectors of scalp EEG epochs associated with SZ and NS classes are randomly divided into ten subsets. Nine subsets of feature vectors are used as a training set while another subset of feature vectors being used as a testing set. This process is repeated ten times with each of the ten subsets of feature vectors being used once as the training set. The performance of tenfold cross-validation is determined from all ten classifications.

The performance of epileptic seizure classifications is evaluated using three conventional classification performance measures: accuracy, sensitivity, and specificity. The accuracy (Ac), the sensitivity (Se), and the specificity (Sp) are given, respectively, by

$$\mathrm{Ac} = \frac{\mathrm{TP} + \mathrm{TN}}{\mathrm{TP} + \mathrm{TN} + \mathrm{FP} + \mathrm{FN}}$$

$$\mathrm{Se} = \frac{\mathrm{TP}}{\mathrm{TP} + \mathrm{FN}}, \text{ and}$$

$$\mathrm{Sp} = \frac{\mathrm{TN}}{\mathrm{TN} + \mathrm{FP}}$$

where TP, TN, FP, and FN denote a number of true positives, a number of true negatives, a number of false positives, and a number of false negatives, respectively. All channels of bipolar scalp EEG data are analyzed and examined in this study. Nevertheless, only results that are obtained from the channel providing the best performance on epileptic seizure classification for each case with respect to the product of sensitivity and specificity are presented.

In addition, the performance of patient-dependent epileptic seizure classification using the wavelet-based features is compared to that using the best five time-domain

Table 3 Performance on patient-dependent epileptic seizure classification using 2 wavelet-based features

Subject	Channel	Feature	Accuracy (Ac)	Sensitivity (Se)	Specificity (Sp)	Se × Sp
chb01	FT9-FT10	λ_2, λ_5	0.9752	0.9436	0.9767	0.9216
chb02	P7-O1	λ_2, λ_4	0.9915	0.9080	0.9955	0.9040
chb03	T7-FT9	λ_4, λ_5	0.9802	0.9083	0.9831	0.8929
chb04	C4-P4	λ_2, λ_5	0.9523	0.4985	0.9863	0.4916
chb05	P8-O2	λ_5, λ_6	0.9856	0.8966	0.9923	0.8897
chb06	F8-T8	λ_1, λ_3	0.9924	0.4417	0.9980	0.4408
chb07	FP1-F3	λ_2, λ_3	0.9522	0.7106	0.9763	0.6938
chb08	FZ-CZ	λ_4, λ_6	0.9503	0.7297	0.9809	0.7158
chb09	C3-P3	λ_2, λ_4	0.9978	0.9806	0.9987	0.9793
chb10	F7-T7	λ_4, λ_5	0.9898	0.7875	0.9998	0.7873
chb11	F7-T7	λ_3, λ_4	0.9071	0.6513	0.9783	0.6371
chb12	F8-T8	λ_2, λ_4	0.9584	0.2515	0.9972	0.2508
chb13	FZ-CZ	λ_2, λ_6	0.8425	0.5522	0.8538	0.4715
chb14	C4-P4	λ_2, λ_6	0.9900	0.3617	0.9992	0.3614
chb15	T7-P7	λ_5, λ_7	0.9629	0.8628	0.9714	0.8381
chb16	C4-P4	λ_2, λ_4	0.9847	0.1754	0.9893	0.1736
chb17	CZ-PZ	λ_3, λ_4	0.9727	0.8794	0.9808	0.8625
chb18	P8-O2	λ_6, λ_7	0.9561	0.7041	0.9671	0.6809
chb19	P8-O2	λ_3, λ_4	0.9826	0.8831	0.9899	0.8742
chb20	C3-P3	λ_2, λ_4	0.9860	0.7570	0.9920	0.7509
chb21	CZ-PZ	λ_1, λ_3	0.9819	0.8029	0.9882	0.7935
chb22	F3-C3	λ_4, λ_5	0.9896	0.9155	0.9937	0.9097
chb23	T7-P7	λ_4, λ_5	0.9791	0.8863	0.9826	0.8709
chb24	FZ-CZ	λ_2, λ_4	0.9704	0.7917	0.9757	0.7724
Average			0.9680	0.7200	0.9811	0.7069

Table 4 Performance on patient-dependent epileptic seizure classification using 3 wavelet-based features

Subject	Channel	Feature	Accuracy (Ac)	Sensitivity (Se)	Specificity (Sp)	Se ×Sp
chb01	FT9-FT10	$\lambda_2, \lambda_3, \lambda_5$	0.9790	0.8923	0.9833	0.8774
chb02	F3-C3	$\lambda_2, \lambda_4, \lambda_5$	0.9760	0.9195	0.9787	0.9000
chb03	T7-FT9	$\lambda_3, \lambda_4, \lambda_5$	0.9796	0.8757	0.9838	0.8615
chb04	C4-P4	$\lambda_2, \lambda_3, \lambda_5$	0.9471	0.4025	0.9879	0.3976
chb05	FP1-F7	$\lambda_4, \lambda_5, \lambda_6$	0.9785	0.7448	0.9962	0.7420
chb06	F8-T8	$\lambda_1, \lambda_2, \lambda_3$	0.9924	0.4167	0.9983	0.4160
chb07	FP1-F3	$\lambda_1, \lambda_2, \lambda_3$	0.9449	0.5787	0.9813	0.5679
chb08	FZ-CZ	$\lambda_4, \lambda_5, \lambda_6$	0.9508	0.7351	0.9807	0.7210
chb09	F7-T7	$\lambda_2, \lambda_3, \lambda_4$	0.9964	0.9660	0.9980	0.9641
chb10	F7-T7	$\lambda_3, \lambda_4, \lambda_5$	0.9814	0.6075	0.9998	0.6074
chb11	FT9-FT10	$\lambda_2, \lambda_3, \lambda_4$	0.8851	0.4795	0.9979	0.4785
chb12	C4-P4	$\lambda_1, \lambda_3, \lambda_4$	0.9687	0.4139	0.9992	0.4136
chb13	FZ-CZ	$\lambda_2, \lambda_5, \lambda_6$	0.8738	0.4776	0.8892	0.4247
chb14	CZ-PZ	$\lambda_1, \lambda_2, \lambda_3$	0.9807	0.3191	0.9904	0.3161
chb15	T7-P7	$\lambda_5, \lambda_7, \lambda_8$	0.9571	0.7797	0.9722	0.7579
chb16	F4-C4	$\lambda_1, \lambda_3, \lambda_4$	0.9937	0.1930	0.9983	0.1927
chb17	CZ-PZ	$\lambda_2, \lambda_3, \lambda_4$	0.9679	0.9246	0.9717	0.8984
chb18	C4-P4	$\lambda_2, \lambda_3, \lambda_6$	0.9652	0.5655	0.9826	0.5557
chb19	P8-O2	$\lambda_2, \lambda_3, \lambda_4$	0.9822	0.8312	0.9933	0.8256
chb20	C3-P3	$\lambda_1, \lambda_2, \lambda_3$	0.9875	0.7450	0.9938	0.7404
chb21	CZ-PZ	$\lambda_1, \lambda_2, \lambda_5$	0.9844	0.8029	0.9908	0.7955
chb22	F3-C3	$\lambda_2, \lambda_4, \lambda_5$	0.9907	0.8803	0.9969	0.8775
chb23	T7-P7	$\lambda_4, \lambda_5, \lambda_6$	0.9818	0.8462	0.9870	0.8351
chb24	FZ-CZ	$\lambda_2, \lambda_3, \lambda_4$	0.9734	0.7829	0.9791	0.7665
Average			0.9674	0.6742	0.9846	0.6742

features [9], i.e., line length, nonlinear energy, variance, power, and maximum, in terms of the area under ROC curve (AUC). Also, the accuracy, the sensitivity and the specificity obtained from patient-dependent epileptic seizure classification using SVM are compared. The line length f_1, nonlinear energy f_2, variance f_3, power f_4, and maximum f_5 are, respectively, defined as follows [9]:

$$f_1 = \sum_{n=1}^{N-1} \left| x[n-1] - x[n] \right| \tag{7}$$

$$f_2 = \frac{1}{N-2} \sum_{n=1}^{N-2} x^2[n] - x[n-1]x[n+1] \tag{8}$$

$$f_3 = \frac{1}{N} \sum_{n=0}^{N-1} (x[n] - \bar{x})^2 \tag{9}$$

$$f_4 = \frac{1}{N} \sum_{n=0}^{N-1} x^2[n] \tag{10}$$

$$f_5 = \max(x[n]) \tag{11}$$

where N denotes the length of EEG signal $x[n]$ and $\bar{x}$ denotes the mean of $x[n]$.

3 Results

3.1 Characteristics of wavelet-based features

Means and standard deviations of all wavelet-based features, i.e., λ_1, λ_2, λ_3, λ_4, λ_5, λ_6, λ_7, and λ_8, of both SZ and NS epochs for each case are summarized in Table 2. The characteristics of wavelet-based features vary corresponding to cases and also subbands. In general, wavelet-based features λ_i of SZ epochs tend to be higher than those of NS epochs. From the results of two-sample t-tests (p-value of 0.0001), it is suggested that for all cases there is at least one wavelet-based feature that associates with the significant difference between the means of corresponding wavelet-based features of both SZ and NS epochs. The means of any wavelet-based feature, i.e., λ_1, λ_2, λ_3, λ_4, λ_5, λ_6, λ_7, and λ_8, of SZ epochs are significantly different from those of NS epochs in 13 cases (chb01, chb03, chb05, chb07, chb08, chb09, chb11, chb17, chb18, chb21,

Table 5 Performance on patient-dependent epileptic seizure classification using 4 wavelet-based features

Subject	Channel	Feature	Accuracy (Ac)	Sensitivity (Se)	Specificity (Sp)	Se × Sp
chb01	FT9-FT10	$\lambda_1, \lambda_2, \lambda_3, \lambda_4$	0.9824	0.7333	0.9948	0.7295
chb02	F3-C3	$\lambda_3, \lambda_4, \lambda_5, \lambda_8$	0.9754	0.7931	0.9843	0.7807
chb03	T7-FT9	$\lambda_1, \lambda_2, \lambda_3, \lambda_4$	0.9678	0.7781	0.9755	0.7590
chb04	FZ-CZ	$\lambda_3, \lambda_4, \lambda_5, \lambda_7$	0.9400	0.2477	0.9919	0.2457
chb05	FZ-CZ	$\lambda_1, \lambda_2, \lambda_3, \lambda_4$	0.9659	0.6207	0.9920	0.6157
chb06	T7-FT9	$\lambda_1, \lambda_2, \lambda_3, \lambda_4$	0.9910	0.3750	0.9974	0.3740
chb07	FP1-F3	$\lambda_1, \lambda_2, \lambda_3, \lambda_4$	0.9341	0.4638	0.9809	0.4550
chb08	T8-P8	$\lambda_2, \lambda_4, \lambda_5, \lambda_6$	0.9462	0.6878	0.9820	0.6755
chb09	C3-P3	$\lambda_2, \lambda_3, \lambda_4, \lambda_5$	0.9940	0.9078	0.9985	0.9064
chb10	F7-T7	$\lambda_2, \lambda_3, \lambda_4, \lambda_5$	0.9711	0.3850	0.9999	0.3850
chb11	FT9-FT10	$\lambda_2, \lambda_3, \lambda_4, \lambda_6$	0.8664	0.3936	0.9979	0.3927
chb12	C4-P4	$\lambda_1, \lambda_2, \lambda_3, \lambda_4$	0.9691	0.4214	0.9992	0.4211
chb13	FZ-CZ	$\lambda_2, \lambda_3, \lambda_5, \lambda_6$	0.8925	0.3945	0.9119	0.3597
chb14	C4-P4	$\lambda_1, \lambda_2, \lambda_3, \lambda_6$	0.9886	0.2128	0.9999	0.2127
chb15	T7-P7	$\lambda_4, \lambda_5, \lambda_6, \lambda_7$	0.9402	0.5653	0.9721	0.5495
chb16	F4-C4	$\lambda_1, \lambda_2, \lambda_3, \lambda_4$	0.9944	0.1579	0.9992	0.1578
chb17	CZ-PZ	$\lambda_2, \lambda_3, \lambda_4, \lambda_7$	0.9671	0.8241	0.9795	0.8072
chb18	CZ-PZ	$\lambda_2, \lambda_3, \lambda_5, \lambda_6$	0.9534	0.5094	0.9728	0.4955
chb19	FP2-F4	$\lambda_1, \lambda_2, \lambda_3, \lambda_4$	0.9822	0.7727	0.9976	0.7709
chb20	F3-C3	$\lambda_1, \lambda_2, \lambda_3, \lambda_5$	0.9883	0.6295	0.9977	0.6280
chb21	CZ-PZ	$\lambda_1, \lambda_2, \lambda_4, \lambda_5$	0.9807	0.7956	0.9872	0.7854
chb22	FZ-CZ	$\lambda_1, \lambda_2, \lambda_4, \lambda_5$	0.9899	0.8732	0.9965	0.8701
chb23	P3-O1	$\lambda_2, \lambda_3, \lambda_5, \lambda_6$	0.9833	0.8161	0.9897	0.8076
chb24	FZ-CZ	$\lambda_1, \lambda_2, \lambda_3, \lambda_4$	0.9824	0.6491	0.9923	0.6441
Average			0.9644	0.5836	0.9871	0.5762

chb22, chb23, and chb24). On the contrary, for the case chb06, there is a significant difference between the means of only wavelet-based feature λ_4 of both SZ and NS epochs.

All wavelet-based features of all SZ and NS epochs obtained from all subjects are compared in box plots shown in Fig. 1. This obviously shows the tendency of higher values of wavelet-based features of SZ epochs compared to those of NS epochs. In addition, Figs. 2 and 3, respectively, compare all wavelet-based features of all SZ and NS epochs obtained from the case chb09 posing the best performance on epileptic seizure classification and the case chb16 posing the worst performance on epileptic seizure classification. Figure 2 shows that wavelet-based features of SZ epochs are substantially higher than those of NS epochs in the case chb09. On the other hand, even though wavelet-based features of SZ epochs tend to be higher than those of NS epochs in the case chb16, wavelet-based features of SZ epochs are in the spans of wavelet-based features of NS epochs.

3.2 Performance of patient-dependent epileptic seizure classification

The performances on patient-dependent epileptic seizure classification using the feature vectors composing of 2, 3, 4, 5, 6, and 7 wavelet-based features of scalp EEG epochs corresponding to the first epileptic seizure event as the training data set are shown in Tables 3, 4, 5, 6, 7, and 8, respectively. The EEG channels and the wavelet-based features that provide the best performance on corresponding epileptic seizure classification are individually reported for each case. Remark that the EEG channel slightly changes from case to case. The performance on epileptic seizure classification tends to decrease as the number of wavelet-based features used as the feature vector increases. The wavelet-based features providing the best performance on epileptic seizure classification also vary from case to case.

The best overall performance on patient-dependent epileptic seizure classification is obtained using the feature vector composing of 2 wavelet-based features. There are 19

Table 6 Performance on patient-dependent epileptic seizure classification using 5 wavelet-based features

Subject	Channel	Feature	Accuracy (Ac)	Sensitivity (Se)	Specificity (Sp)	Se × Sp
chb01	FT9-FT10	$\lambda_1, \lambda_2, \lambda_3, \lambda_4, \lambda_5$	0.9760	0.5487	0.9972	0.5472
chb02	FZ-CZ	$\lambda_1, \lambda_2, \lambda_3, \lambda_4, \lambda_5$	0.9770	0.7011	0.9905	0.6945
chb03	T7-FT9	$\lambda_1, \lambda_2, \lambda_3, \lambda_4, \lambda_5$	0.9784	0.6775	0.9906	0.6712
chb04	FZ-CZ	$\lambda_3, \lambda_4, \lambda_5, \lambda_7, \lambda_8$	0.9369	0.1176	0.9984	0.1175
chb05	FZ-CZ	$\lambda_1, \lambda_2, \lambda_3, \lambda_4, \lambda_5$	0.9625	0.5333	0.9950	0.5306
chb06	T8-P8	$\lambda_1, \lambda_2, \lambda_3, \lambda_4, \lambda_5$	0.9888	0.2583	0.9962	0.2574
chb07	FP1-F3	$\lambda_1, \lambda_2, \lambda_3, \lambda_4, \lambda_5$	0.9306	0.3191	0.9915	0.3164
chb08	T8-P8	$\lambda_2, \lambda_3, \lambda_4, \lambda_5, \lambda_6$	0.9423	0.6297	0.9856	0.6206
chb09	F4-C4	$\lambda_1, \lambda_2, \lambda_3, \lambda_4, \lambda_5$	0.9857	0.7476	0.9982	0.7462
chb10	F7-T7	$\lambda_2, \lambda_3, \lambda_4, \lambda_5, \lambda_6$	0.9640	0.2300	1.0000	0.2300
chb11	FT9-FT10	$\lambda_1, \lambda_2, \lambda_3, \lambda_4, \lambda_5$	0.8427	0.2795	0.9993	0.2793
chb12	C4-P4	$\lambda_1, \lambda_2, \lambda_3, \lambda_4, \lambda_7$	0.9584	0.2073	0.9996	0.2073
chb13	FZ-CZ	$\lambda_2, \lambda_3, \lambda_4, \lambda_5, \lambda_6$	0.9095	0.3348	0.9318	0.3119
chb14	FZ-CZ	$\lambda_1, \lambda_2, \lambda_3, \lambda_5, \lambda_7$	0.9869	0.1418	0.9993	0.1417
chb15	C3-P3	$\lambda_1, \lambda_2, \lambda_3, \lambda_4, \lambda_5$	0.9110	0.3855	0.9556	0.3684
chb16	F4-C4	$\lambda_1, \lambda_2, \lambda_3, \lambda_4, \lambda_6$	0.9947	0.0877	0.9999	0.0877
chb17	CZ-PZ	$\lambda_2, \lambda_3, \lambda_4, \lambda_5, \lambda_7$	0.9631	0.6784	0.9878	0.6701
chb18	CZ-PZ	$\lambda_2, \lambda_3, \lambda_4, \lambda_5, \lambda_6$	0.9633	0.4120	0.9873	0.4067
chb19	FP2-F4	$\lambda_1, \lambda_2, \lambda_3, \lambda_4, \lambda_5$	0.9634	0.4675	1.0000	0.4675
chb20	F3-C3	$\lambda_1, \lambda_2, \lambda_3, \lambda_4, \lambda_5$	0.9861	0.4741	0.9996	0.4739
chb21	CZ-PZ	$\lambda_1, \lambda_2, \lambda_3, \lambda_4, \lambda_5$	0.9802	0.7372	0.9887	0.7289
chb22	FZ-CZ	$\lambda_1, \lambda_2, \lambda_3, \lambda_4, \lambda_5$	0.9892	0.8310	0.9980	0.8294
chb23	P3-O1	$\lambda_1, \lambda_2, \lambda_3, \lambda_5, \lambda_6$	0.9806	0.7391	0.9898	0.7316
chb24	FZ-CZ	$\lambda_1, \lambda_2, \lambda_3, \lambda_4, \lambda_5$	0.9791	0.3487	0.9978	0.3479
Average			0.9604	0.4537	0.9907	0.4493

cases that the feature vector composing of 2 wavelet-based features provides the best performance on epileptic seizure classification. The best performance on patient-dependent epileptic seizure classification is obtained using the feature vector composing of 3 wavelet-based features for the cases chb10, chb16, chb17, and chb21. The feature vector composing of 4 wavelet-based features is required to obtain the best performance on patient-dependent epileptic seizure classification for the case chb12. The best performances on patient-dependent epileptic seizure classification for each case are summarized in Table 9.

The best performance on patient-dependent epileptic seizure classification is obtained at the case chb09 which corresponds to the accuracy of 0.9978, the sensitivity of 0.9806, and the specificity of 0.9987 using the wavelet-based features λ_2 and λ_4 as the feature vector. The worst performance on patient-dependent epileptic seizure classification is obtained at the case chb16 which corresponds to the accuracy of 0.9937, the sensitivity of 0.1930, and the specificity of 0.9983 using the wavelet-based features λ_1, λ_3 and λ_4 as the feature vector. The distributions of wavelet-based features of both SZ and NS epochs corresponding to each epileptic seizure event of cases chb09 and chb16 are compared in box plots shown in Figs. 4 and 5, respectively. These obviously give a justification for the corresponding performances. The wavelet-based features of SZ and NS epochs in the case chb09 slightly vary from one epileptic seizure event to another for all four epileptic seizure events. There are, however, considerable variations on wavelet-based features of SZ and NS epochs within ten epileptic seizure events for the case chb16. Furthermore, in the case of chb16 the range of wavelet-based features of NS epochs is over that of wavelet-based features of SZ epochs. This makes such epileptic seizure classification unfeasible.

3.3 Performance evaluation using tenfold cross-validation

Using the same corresponding EEG channels and wavelet-based features providing the best performance reported in Table 3, the results of tenfold cross-validation on patient-dependent epileptic seizure classification are summarized in Table 10. In general, the accuracy and the specificity of patient-dependent epileptic seizure classification are remarkably high. Both accuracy and specificity are higher than 0.90 for all cases. The highest and lowest accuracies

Table 7 Performance on patient-dependent epileptic seizure classification using 6 wavelet-based features

Subject	Channel	Feature	Accuracy (Ac)	Sensitivity (Se)	Specificity (Sp)	Se × Sp
chb01	FZ-CZ	$\lambda_1, \lambda_2, \lambda_3, \lambda_4, \lambda_5, \lambda_6$	0.9675	0.3974	0.9958	0.3958
chb02	F7-T7	$\lambda_1, \lambda_2, \lambda_3, \lambda_4, \lambda_5, \lambda_6$	0.9712	0.3793	1.0000	0.3793
chb03	T7-FT9	$\lambda_1, \lambda_2, \lambda_3, \lambda_4, \lambda_5, \lambda_6$	0.9744	0.4320	0.9964	0.4304
chb04	T7-FT9	$\lambda_1, \lambda_2, \lambda_3, \lambda_4, \lambda_5, \lambda_7$	0.9337	0.0650	0.9988	0.0649
chb05	FZ-CZ	$\lambda_1, \lambda_2, \lambda_3, \lambda_4, \lambda_5, \lambda_6$	0.9536	0.3586	0.9986	0.3581
chb06	T8-P8	$\lambda_1, \lambda_2, \lambda_3, \lambda_4, \lambda_5, \lambda_6$	0.9899	0.1250	0.9987	0.1248
chb07	FP1-F3	$\lambda_1, \lambda_2, \lambda_3, \lambda_4, \lambda_5, \lambda_6$	0.9171	0.1319	0.9953	0.1313
chb08	FZ-CZ	$\lambda_1, \lambda_2, \lambda_3, \lambda_4, \lambda_5, \lambda_6$	0.9294	0.5662	0.9798	0.5548
chb09	F4-C4	$\lambda_1, \lambda_2, \lambda_3, \lambda_4, \lambda_5, \lambda_6$	0.9717	0.4466	0.9992	0.4463
chb10	C3-P3	$\lambda_1, \lambda_2, \lambda_3, \lambda_4, \lambda_5, \lambda_6$	0.9587	0.1600	0.9979	0.1597
chb11	FZ-CZ	$\lambda_1, \lambda_2, \lambda_3, \lambda_4, \lambda_5, \lambda_6$	0.8173	0.1654	0.9986	0.1651
chb12	F4-C4	$\lambda_1, \lambda_2, \lambda_3, \lambda_4, \lambda_5, \lambda_7$	0.9513	0.0883	0.9987	0.0882
chb13	FZ-CZ	$\lambda_2, \lambda_3, \lambda_4, \lambda_5, \lambda_6, \lambda_7$	0.9421	0.1620	0.9724	0.1576
chb14	FZ-CZ	$\lambda_1, \lambda_2, \lambda_3, \lambda_4, \lambda_5, \lambda_7$	0.9865	0.0922	0.9996	0.0922
chb15	P7-O1	$\lambda_2, \lambda_3, \lambda_4, \lambda_5, \lambda_6, \lambda_7$	0.9380	0.2603	0.9956	0.2591
chb16	F4-C4	$\lambda_1, \lambda_2, \lambda_3, \lambda_4, \lambda_6, \lambda_8$	0.9945	0.0351	1.0000	0.0351
chb17	CZ-PZ	$\lambda_2, \lambda_3, \lambda_4, \lambda_5, \lambda_6, \lambda_7$	0.9410	0.3869	0.9891	0.3827
chb18	CZ-PZ	$\lambda_2, \lambda_3, \lambda_4, \lambda_5, \lambda_6, \lambda_7$	0.9658	0.2772	0.9958	0.2760
chb19	F7-T7	$\lambda_1, \lambda_2, \lambda_3, \lambda_4, \lambda_5, \lambda_6$	0.9433	0.1818	0.9995	0.1817
chb20	F3-C3	$\lambda_1, \lambda_2, \lambda_3, \lambda_4, \lambda_5, \lambda_6$	0.9800	0.2271	0.9998	0.2270
chb21	CZ-PZ	$\lambda_1, \lambda_2, \lambda_3, \lambda_4, \lambda_5, \lambda_6$	0.9802	0.6423	0.9921	0.6372
chb22	FZ-CZ	$\lambda_1, \lambda_2, \lambda_3, \lambda_4, \lambda_5, \lambda_8$	0.9773	0.5775	0.9996	0.5772
chb23	P4-O2	$\lambda_1, \lambda_2, \lambda_3, \lambda_4, \lambda_5, \lambda_6$	0.9595	0.6421	0.9717	0.6239
chb24	FZ-CZ	$\lambda_1, \lambda_2, \lambda_3, \lambda_4, \lambda_5, \lambda_6$	0.9766	0.2018	0.9997	0.2017
Average			0.9550	0.2918	0.9947	0.2896

are, respectively, 0.9959 and 0.9281 while the highest and lowest specificities are, respectively, 0.9997 and 0.9910. On the contrary, the wide range of sensitivity is obtained. The best and worst sensitivities are 0.9295 and 0.0174, respectively. The performance on patient-dependent epileptic seizure classification evaluated using tenfold cross-validation is in general lower than those using the wavelet-based features of scalp EEG epochs corresponding to the first epileptic seizure event as the training data set. The better performance on patient-dependent epileptic seizure classification evaluated using tenfold cross-validation is achieved in the cases chb04, chb10, chb11, chb14, and chb22.

The results of tenfold cross-validation on the patient-independent epileptic seizure classification corresponding to each pair of wavelet-based features are summarized in Table 11. The same EEG channels providing the best performance for all cases reported in Table 3 are used. The highest product of sensitivity and specificity is 0.2004 that is obtained from the patient-independent epileptic seizure classification using the wavelet-based features λ_1 and λ_5 as the feature vector. The corresponding accuracy, sensitivity, and specificity are 0.9579, 0.2011, and 0.9965, respectively. On the other hand, the worst performance on the patient-independent epileptic seizure classification is obtained using the wavelet-based features λ_7 and λ_8 as the feature vector with the accuracy, sensitivity, and specificity of 0.9518, 0.0259, and 0.9990, respectively.

3.4 Comparison of performance on patient-dependent epileptic seizure classification

The areas under ROC curve obtained from using the wavelet-based features and the time-domain features are compared in Table 12. The maximum area under ROC curve for each case is written in bold. In general, the wavelet-based features provide better performance on epileptic seizure classification compared to the time-domain features. The wavelet-based features, i.e., λ_3, λ_4, λ_5, and λ_6, provide the best classification performance regarding to the maximum area under ROC curve in 18 cases while the time-domain features, i.e., f_2, f_4, and f_5

Table 8 Performance on patient-dependent epileptic seizure classification using 7 wavelet-based features

Subject	Channel	Feature	Accuracy (Ac)	Sensitivity (Se)	Specificity (Sp)	Se × Sp
chb01	FZ-CZ	$\lambda_1, \lambda_2, \lambda_3, \lambda_4, \lambda_5, \lambda_6, \lambda_7$	0.9598	0.1513	0.9999	0.1513
chb02	P3-O1	$\lambda_1, \lambda_2, \lambda_3, \lambda_4, \lambda_5, \lambda_6, \lambda_7$	0.9599	0.1609	0.9989	0.1607
chb03	T7-FT9	$\lambda_1, \lambda_2, \lambda_3, \lambda_4, \lambda_5, \lambda_6, \lambda_7$	0.9660	0.1361	0.9996	0.1360
chb04	C3-P3	$\lambda_1, \lambda_2, \lambda_3, \lambda_4, \lambda_5, \lambda_6, \lambda_7$	0.9313	0.0217	0.9995	0.0217
chb05	FZ-CZ	$\lambda_1, \lambda_2, \lambda_3, \lambda_4, \lambda_5, \lambda_6, \lambda_8$	0.9388	0.1356	0.9997	0.1356
chb06	T8-P8	$\lambda_1, \lambda_2, \lambda_3, \lambda_4, \lambda_5, \lambda_6, \lambda_8$	0.9904	0.0583	0.9999	0.0583
chb07	FP1-F3	$\lambda_1, \lambda_2, \lambda_3, \lambda_4, \lambda_5, \lambda_6, \lambda_7$	0.9113	0.0426	0.9979	0.0425
chb08	CZ-PZ	$\lambda_1, \lambda_2, \lambda_3, \lambda_4, \lambda_5, \lambda_6, \lambda_7$	0.9181	0.4135	0.9880	0.4086
chb09	T7-FT9	$\lambda_1, \lambda_2, \lambda_3, \lambda_4, \lambda_5, \lambda_6, \lambda_7$	0.9589	0.1748	1.0000	0.1748
chb10	F3-C3	$\lambda_1, \lambda_2, \lambda_3, \lambda_4, \lambda_5, \lambda_6, \lambda_7$	0.9529	0.0900	0.9952	0.0896
chb11	FZ-CZ	$\lambda_2, \lambda_3, \lambda_4, \lambda_5, \lambda_6, \lambda_7, \lambda_8$	0.7858	0.0154	1.0000	0.0154
chb12	F4-C4	$\lambda_1, \lambda_2, \lambda_3, \lambda_4, \lambda_5, \lambda_6, \lambda_7$	0.9487	0.0329	0.9989	0.0329
chb13	FZ-CZ	$\lambda_1, \lambda_2, \lambda_3, \lambda_4, \lambda_5, \lambda_6, \lambda_7$	0.9517	0.0768	0.9857	0.0757
chb14	C3-P3	$\lambda_1, \lambda_2, \lambda_3, \lambda_4, \lambda_5, \lambda_6, \lambda_7$	0.9860	0.0284	1.0000	0.0284
chb15	P7-O1	$\lambda_1, \lambda_2, \lambda_3, \lambda_4, \lambda_5, \lambda_6, \lambda_7$	0.9298	0.1258	0.9982	0.1255
chb16	FP2-F8	$\lambda_1, \lambda_2, \lambda_3, \lambda_4, \lambda_5, \lambda_6, \lambda_8$	0.9944	0.0175	1.0000	0.0175
chb17	F3-C3	$\lambda_1, \lambda_2, \lambda_3, \lambda_4, \lambda_5, \lambda_6, \lambda_7$	0.9262	0.1307	0.9952	0.1300
chb18	FZ-CZ	$\lambda_1, \lambda_2, \lambda_3, \lambda_4, \lambda_5, \lambda_6, \lambda_7$	0.9503	0.1199	0.9865	0.1182
chb19	F8-T8	$\lambda_1, \lambda_2, \lambda_3, \lambda_4, \lambda_5, \lambda_6, \lambda_7$	0.9335	0.0325	1.0000	0.0325
chb20	CZ-PZ	$\lambda_1, \lambda_2, \lambda_3, \lambda_4, \lambda_5, \lambda_6, \lambda_7$	0.9756	0.0558	0.9998	0.0558
chb21	CZ-PZ	$\lambda_1, \lambda_2, \lambda_3, \lambda_4, \lambda_5, \lambda_6, \lambda_7$	0.9757	0.4015	0.9959	0.3998
chb22	FZ-CZ	$\lambda_1, \lambda_2, \lambda_3, \lambda_4, \lambda_5, \lambda_6, \lambda_7$	0.9597	0.2465	0.9996	0.2464
chb23	P4-O2	$\lambda_1, \lambda_2, \lambda_3, \lambda_4, \lambda_5, \lambda_6, \lambda_8$	0.9659	0.3612	0.9890	0.3572
chb24	FZ-CZ	$\lambda_1, \lambda_2, \lambda_3, \lambda_4, \lambda_5, \lambda_6, \lambda_7$	0.9727	0.0570	1.0000	0.0570
Average			0.9476	0.1286	0.9970	0.1280

provide the best classification in the other 6 cases. The wavelet-based features λ_4 and λ_5 are the wavelet-based features providing the best classification performance among all eight wavelet-based features. The nonlinear energy, i.e., f_2, is the time-domain feature providing the best classification performance among all five time-domain features.

Table 13 shows the best performance on patient-dependent epileptic seizure classification using the time-domain features and SVM. The best performance on patient-dependent epileptic seizure classification can be achieved using the feature vector composing of 2, 3, and 4 time-domain features for 13, 7, and 4 cases, respectively. The best performance is obtained at the case chb09 using the line length, the nonlinear energy, the variance, and the maximum as the feature vector while the worst performance is obtained at the case chb16 using the line length and the variance as the feature vector. In general, the wavelet-based features provide the better performance for epileptic seizure classification than the time-domain features. The better performance on patient-dependent epileptic seizure classification can be obtained using the wavelet-based features in 19 cases.

4 Discussion

From the computational results, it is shown that, in general, the wavelet-based features of scalp EEG epochs associated with epileptic seizure event and non-seizure period, i.e., pre-ictal and post-ictal states, are considerably different from each other corresponding to the same case. Furthermore, this suggests that at any spectral subband the power of scalp EEG epochs associated with epileptic seizure event is higher than those of scalp EEG epochs associated with non-seizure period. Such differences between the wavelet-based features lead to an excellent epileptic seizure classification. The average accuracy, sensitivity, and specificity of patient-dependent epileptic seizure classification are, respectively, 0.9680, 0.7200, and 0.9811. This performance is comparable with the computational results of the automated patient-dependent epileptic seizure classification [7] where the corresponding average sensitivity and specificity are 89.01 and 94.71%. However, a larger number of quantitative features were applied in Ref. [7]. The best accuracy, sensitivity, and specificity of patient-dependent epileptic seizure classification are 0.9978, 0.9806, and 0.9998, respectively.

Table 9 Best performance on patient-dependent epileptic seizure classification

Subject	Channel	Feature	Accuracy (Ac)	Sensitivity (Se)	Specificity (Sp)	Se × Sp
chb01	FT9-FT10	λ_2, λ_5	0.9752	0.9436	0.9767	0.9216
chb02	P7-O1	λ_2, λ_4	0.9915	0.9080	0.9955	0.9040
chb03	T7-FT9	λ_4, λ_5	0.9802	0.9083	0.9831	0.8929
chb04	C4-P4	λ_2, λ_5	0.9523	0.4985	0.9863	0.4916
chb05	P8-O2	λ_5, λ_6	0.9856	0.8966	0.9923	0.8897
chb06	F8-T8	λ_1, λ_3	0.9924	0.4417	0.9980	0.4408
chb07	FP1-F3	λ_2, λ_3	0.9522	0.7106	0.9763	0.6938
chb08	FZ-CZ	$\lambda_4, \lambda_5, \lambda_6$	0.9508	0.7351	0.9807	0.7210
chb09	C3-P3	λ_2, λ_4	0.9978	0.9806	0.9987	0.9793
chb10	F7-T7	λ_4, λ_5	0.9898	0.7875	0.9998	0.7873
chb11	F7-T7	λ_3, λ_4	0.9071	0.6513	0.9783	0.6371
chb12	C4-P4	$\lambda_1, \lambda_2, \lambda_3, \lambda_4$	0.9691	0.4214	0.9992	0.4211
chb13	FZ-CZ	λ_2, λ_6	0.8425	0.5522	0.8538	0.4715
chb14	C4-P4	λ_2, λ_6	0.9900	0.3617	0.9992	0.3614
chb15	T7-P7	λ_5, λ_7	0.9629	0.8628	0.9714	0.8381
chb16	F4-C4	$\lambda_1, \lambda_3, \lambda_4$	0.9937	0.1930	0.9983	0.1927
chb17	CZ-PZ	$\lambda_2, \lambda_3, \lambda_4$	0.9679	0.9246	0.9717	0.8984
chb18	P8-O2	λ_6, λ_7	0.9561	0.7041	0.9671	0.6809
chb19	P8-O2	λ_3, λ_4	0.9826	0.8831	0.9899	0.8742
chb20	C3-P3	λ_2, λ_4	0.9860	0.7570	0.9920	0.7509
chb21	CZ-PZ	$\lambda_1, \lambda_2, \lambda_5$	0.9844	0.8029	0.9908	0.7955
chb22	F3-C3	λ_4, λ_5	0.9896	0.9155	0.9937	0.9097
chb23	T7-P7	λ_4, λ_5	0.9791	0.8863	0.9826	0.8709
chb24	FZ-CZ	λ_2, λ_4	0.9704	0.7917	0.9757	0.7724
Average			0.9687	0.7299	0.9813	0.7165

A variety of wavelet-based features of scalp EEG epochs are incorporated in the feature vectors used to obtained the best performance on patient-dependent epileptic seizure classification for corresponding cases. The number of wavelet-based features of scalp EEG epochs used to obtained the best performance on patient-dependent epileptic seizure classification also varies among cases. Two wavelet-based features of scalp EEG epochs are required to obtain the best patient-dependent epileptic seizure classification in most cases, i.e., 19 cases out of 24. The wavelet-based features λ_4, λ_2, and λ_5 are the wavelet-based features of scalp EEG epochs that are mostly used as feature vectors to obtain the best performance on patient-dependent epileptic seizure classification. These wavelet-based features, i.e., λ_2, λ_4, and λ_5 correspond to the 32–64, 8–16, and 4–8 Hz subbands of scalp EEG epochs, respectively. The wavelet-based feature λ_8 which corresponds to the 0–1 Hz subband of scalp EEG epochs is not associated with the best performance on patient-dependent epileptic seizure classification of any cases.

The best performance on patient-dependent epileptic seizure classification using the wavelet-based features of scalp EEG epochs corresponding to the first epileptic seizure event as the training data set is achieved with the accuracy of 0.9978, the sensitivity of 0.9806, and the specificity of 0.9987. The accuracy, sensitivity, and specificity of patient-dependent epileptic seizure classification using the wavelet-based features of scalp EEG epochs corresponding to the first epileptic seizure event as the training data set are, respectively, 0.9937, 0.1930, and 0.9983 for the worst performance. The wavelet-based features and the time-domain features provides both best and worst performances on patient-dependent epileptic seizure classification for the same cases. Superior performance of the wavelet-based features for epileptic seizure classification suggests that the distinctive characteristics of epileptic seizure manifest in some specific spectral bands of EEG signals rather than the whole bandwidth of EEG signals.

In the case with best performance on epileptic seizure classification, the consistent characteristics of scalp EEG

Table 10 Performance on patient-dependent epileptic seizure classification using tenfold cross-validation

Subject	Accuracy (Ac)	Sensitivity (Se)	Specificity (Sp)	Se × Sp
chb01	0.9941	0.9081	0.9981	0.9064
chb02	0.9917	0.8628	0.9987	0.8617
chb03	0.9808	0.6057	0.9963	0.6034
chb04	0.9758	0.7165	0.9925	0.7112
chb05	0.9693	0.6405	0.9955	0.6376
chb06	0.9927	0.3576	0.9991	0.3572
chb07	0.9655	0.6343	0.9934	0.6301
chb08	0.9281	0.4116	0.9975	0.4105
chb09	0.9959	0.9295	0.9992	0.9288
chb10	0.9907	0.8001	0.9993	0.7996
chb11	0.9795	0.9247	0.9910	0.9164
chb12	0.9592	0.2566	0.9973	0.2559
chb13	0.9640	0.0622	0.9981	0.0621
chb14	0.9920	0.4604	0.9993	0.4601
chb15	0.9590	0.5457	0.9949	0.5429
chb16	0.9942	0.0174	0.9997	0.0174
chb17	0.9809	0.7995	0.9949	0.7954
chb18	0.9621	0.2649	0.9938	0.2633
chb19	0.9814	0.7758	0.9967	0.7733
chb20	0.9910	0.6695	0.9997	0.6692
chb21	0.9886	0.7917	0.9957	0.7883
chb22	0.9938	0.9293	0.9975	0.9269
chb23	0.9884	0.8138	0.9962	0.8107
chb24	0.9904	0.6755	0.9994	0.6751
Average	0.9796	0.6189	0.9968	0.6168

Table 11 Performance on patient-independent epileptic seizure classification using tenfold cross-validation

Feature	Accuracy (Ac)	Sensitivity (Se)	Specificity (Sp)	Se × Sp
λ_1, λ_2	0.9523	0.0439	0.9987	0.0438
λ_1, λ_3	0.9554	0.1592	0.9960	0.1585
λ_1, λ_4	0.9570	0.1714	0.9971	0.1709
λ_1, λ_5	0.9579	0.2011	0.9965	0.2004
λ_1, λ_6	0.9564	0.1631	0.9969	0.1625
λ_1, λ_7	0.9532	0.0764	0.9980	0.0763
λ_1, λ_8	0.9525	0.0586	0.9982	0.0585
λ_2, λ_3	0.9542	0.1050	0.9976	0.1047
λ_2, λ_4	0.9561	0.1531	0.9970	0.1527
λ_2, λ_5	0.9564	0.1626	0.9969	0.1621
λ_2, λ_6	0.9556	0.1410	0.9972	0.1406
λ_2, λ_7	0.9533	0.0766	0.9980	0.0764
λ_2, λ_8	0.9524	0.0505	0.9984	0.0504
λ_3, λ_4	0.9551	0.1266	0.9974	0.1262
λ_3, λ_5	0.9564	0.1587	0.9971	0.1582
λ_3, λ_6	0.9555	0.1327	0.9975	0.1324
λ_3, λ_7	0.9544	0.1028	0.9979	0.1025
λ_3, λ_8	0.9526	0.0593	0.9982	0.0592
λ_4, λ_5	0.9558	0.1389	0.9975	0.1385
λ_4, λ_6	0.9560	0.1437	0.9975	0.1433
λ_4, λ_7	0.9552	0.1278	0.9974	0.1275
λ_4, λ_8	0.9532	0.0912	0.9972	0.0909
λ_5, λ_6	0.9558	0.1384	0.9976	0.1380
λ_5, λ_7	0.9552	0.1295	0.9974	0.1292
λ_5, λ_8	0.9553	0.1285	0.9975	0.1282
λ_6, λ_7	0.9543	0.1060	0.9976	0.1058
λ_6, λ_8	0.9539	0.0975	0.9976	0.0973
λ_7, λ_8	0.9518	0.0259	0.9990	0.0258

epochs associated with epileptic seizure event and non-seizure periods are observed as their corresponding wavelet-based features are particularly steady among various epileptic seizure events. Furthermore, the durations of epileptic seizure events are sufficiently long. The average duration of 4 epileptic seizure events is 69 s. On the contrary, the characteristics of scalp EEG epochs associated with epileptic seizure event and non-seizure periods relatively vary from one epileptic seizure event to another in the case of worst performance on epileptic seizure classification. The durations of epileptic seizure events are also exceptionally brief. The longest and shortest durations of epileptic seizure events are 14 and 6 s, respectively. This leads to a very small number of scalp EEG epochs associated with epileptic seizure event applied to the classification.

When the tenfold cross-validation is applied, the performance on patient-dependent epileptic seizure classification tends to decrease. In most cases, i.e., 19 cases out of 24, the performance on patient-dependent epileptic seizure classification using tenfold cross-validations is lower than those using the wavelet-based features of scalp EEG epochs corresponding to the first epileptic seizure event. This suggests that the wavelet-based features of scalp EEG epochs obtained from a single event, i.e., around the first epileptic seizure event, may not well represent the whole classes due to the variation of characteristics of scalp EEG epochs associated with epileptic seizure event and non-seizure period from one epileptic seizure event to another. The performance on patient-independent epileptic seizure classification is relatively low compared to the performance on patient-dependent epileptic seizure classification. The variation of characteristics of scalp EEG epochs associated with epileptic

Table 12 Area under ROC curve of patient-dependent epileptic seizure classification

Case	Wavelet-based feature								Time-domain feature				
	λ_1	λ_2	λ_3	λ_4	λ_5	λ_6	λ_7	λ_8	f_1	f_2	f_3	f_4	f_5
chb01	0.882	0.904	0.823	0.868	0.880	0.861	0.823	0.800	0.893	**0.921**	0.876	0.874	0.874
chb02	0.609	0.435	0.547	0.640	0.737	**0.743**	0.666	0.609	0.611	0.602	0.605	0.613	0.593
chb03	0.866	0.881	0.889	0.893	**0.901**	0.858	0.815	0.805	0.880	0.885	0.874	0.872	0.861
chb04	0.840	0.894	0.923	0.950	**0.972**	0.944	0.864	0.793	0.891	0.900	0.921	0.915	0.904
chb05	0.816	0.851	0.902	**0.945**	0.926	0.872	0.814	0.821	0.907	0.918	0.916	0.917	0.907
chb06	0.636	0.677	0.707	0.749	0.720	0.705	0.728	0.704	0.719	0.754	0.768	0.762	**0.775**
chb07	0.934	0.939	0.968	0.971	0.942	0.928	0.905	0.867	0.984	**0.988**	0.930	0.926	0.957
chb08	0.691	0.708	0.813	0.874	0.915	**0.936**	0.882	0.880	0.889	0.887	0.912	0.910	0.882
chb09	0.981	0.989	0.991	**0.993**	0.989	0.957	0.887	0.861	0.977	0.986	0.983	0.983	0.987
chb10	0.849	0.885	0.954	**0.986**	0.983	0.967	0.825	0.815	0.913	0.932	0.976	0.975	0.974
chb11	0.742	0.826	0.920	0.969	**0.978**	0.978	0.949	0.914	0.897	0.893	0.978	0.978	0.955
chb12	0.660	0.682	0.713	**0.741**	0.646	0.583	0.558	0.556	0.711	0.717	0.646	0.644	0.650
chb13	0.521	0.500	0.585	0.672	0.793	**0.871**	0.783	0.681	0.584	0.594	0.847	0.844	0.733
chb14	0.785	0.640	0.773	0.917	**0.947**	0.938	0.888	0.783	0.725	0.766	0.884	0.881	0.876
chb15	0.708	0.826	0.889	**0.907**	0.895	0.801	0.686	0.682	0.834	0.872	0.856	0.853	0.856
chb16	0.709	0.794	**0.883**	0.871	0.799	0.728	0.669	0.737	0.830	0.833	0.804	0.799	0.758
chb17	0.792	0.839	0.883	**0.945**	0.940	0.923	0.842	0.777	0.808	0.847	0.918	0.915	0.904
chb18	0.774	0.791	0.829	0.872	**0.892**	0.890	0.853	0.818	0.846	0.838	0.867	0.868	0.836
chb19	0.808	0.822	0.821	0.844	0.854	0.814	0.753	0.768	0.798	0.801	0.859	**0.859**	0.852
chb20	0.839	0.834	0.841	0.850	0.727	0.712	0.694	0.724	0.855	**0.866**	0.813	0.813	0.812
chb21	0.797	0.953	0.979	0.963	0.954	0.872	0.877	0.835	0.981	**0.983**	0.956	0.953	0.960
chb22	0.848	0.905	0.978	**0.991**	0.990	0.984	0.939	0.904	0.948	0.971	0.989	0.989	0.954
chb23	0.938	0.930	0.927	0.957	**0.978**	0.974	0.963	0.934	0.940	0.937	0.978	0.977	0.959
chb24	0.751	0.798	0.815	**0.818**	0.802	0.802	0.800	0.809	0.795	0.800	0.807	0.808	0.803

seizure event and non-seizure period among cases or subjects is the primary factor of decreasing classification performance. The best performance on patient-independent is achieved using the wavelet-based features λ_1 and λ_5 which correspond to the 64–128 and 4–8 Hz subbands of scalp EEGs. The 64–128 Hz subband of EEGs is associated with high-frequency oscillations, i.e., gamma (30–80 Hz) and ripple (80–250 Hz) oscillations [23]. There is evidence that high-frequency oscillations, in particular, gamma and ripple oscillations, in scalp EEGs are clinically correlated with the seizure onset zone [2, 23].

Table 13 Best performance on patient-dependent epileptic seizure classification using time-domain features

Subject	Channel	Feature	Accuracy (Ac)	Sensitivity (Se)	Specificity (Sp)	Se × Sp
chb01	FT9-FT10	f_1, f_2, f_3	0.9634	0.8923	0.9669	0.8628
chb02	P7-O1	f_1, f_2, f_3	0.9679	0.7816	0.9770	0.7637
chb03	T7-FT9	f_3, f_5	0.9298	0.7426	0.9374	0.6961
chb04	C4-P4	f_1, f_3, f_4, f_5	0.9169	0.3870	0.9566	0.3702
chb05	P8-O2	f_1, f_2	0.9600	0.9701	0.9593	0.9306
chb06	F8-T8	f_1, f_2	0.9939	0.4500	0.9995	0.4498
chb07	FP1-F3	f_2, f_5	0.9688	0.8170	0.9839	0.8039
chb08	FZ-CZ	f_1, f_3, f_4	0.9365	0.6946	0.9700	0.6738
chb09	C3-P3	f_1, f_2, f_3, f_5	0.9855	0.9903	0.9852	0.9757
chb10	F7-T7	f_3, f_4	0.9821	0.9100	0.9856	0.8969
chb11	F7-T7	f_2, f_3, f_4	0.8466	0.3115	0.9954	0.3101
chb12	C4-P4	f_1, f_4	0.9512	0.4162	0.9806	0.4081
chb13	FZ-CZ	f_1, f_2, f_3, f_5	0.9317	0.2601	0.9578	0.2491
chb14	C4-P4	f_3, f_4, f_5	0.9876	0.4043	0.9961	0.4027
chb15	T7-P7	f_3, f_5	0.8177	0.9579	0.8058	0.7718
chb16	F4-C4	f_1, f_3	0.9943	0.0702	0.9996	0.0701
chb17	CZ-PZ	f_3, f_5	0.9306	0.5779	0.9612	0.5555
chb18	P8-O2	f_2, f_3, f_4	0.9419	0.6367	0.9552	0.6082
chb19	P8-O2	f_2, f_3, f_5	0.9639	0.7208	0.9818	0.7077
chb20	C3-P3	f_2, f_5	0.9848	0.7052	0.9921	0.6996
chb21	CZ-PZ	f_2, f_4	0.9804	0.7226	0.9895	0.7150
chb22	F3-C3	f_1, f_2	0.9761	0.8310	0.9843	0.8179
chb23	T7-P7	f_1, f_3, f_4, f_5	0.9683	0.8863	0.9714	0.8609
chb24	FZ-CZ	f_1, f_5	0.9605	0.7873	0.9656	0.7602
Average			0.9517	0.6635	0.9691	0.6400

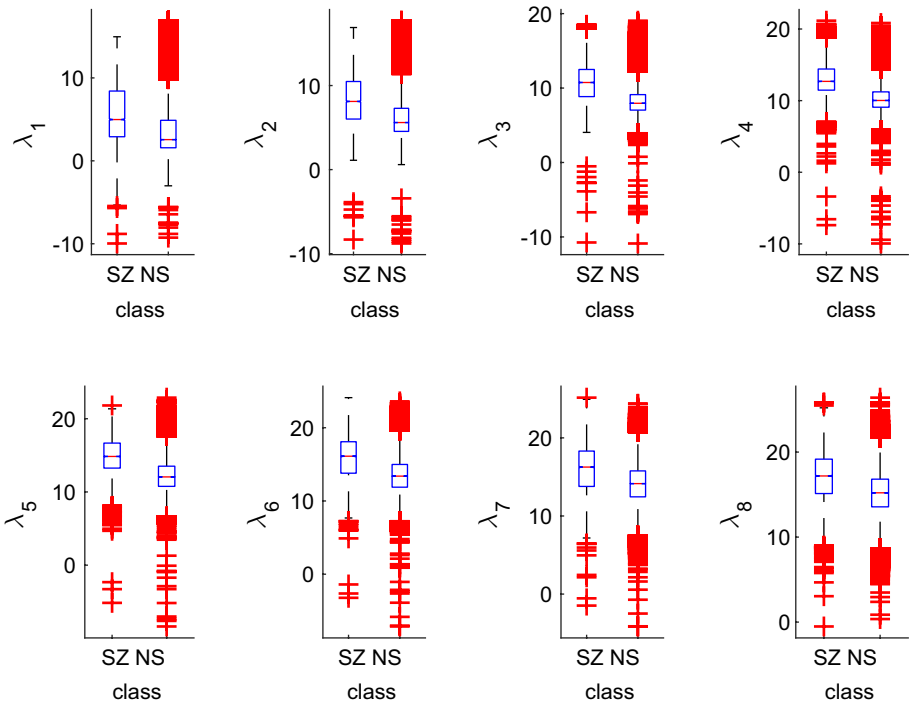

Fig. 1 Comparison between the wavelet-based features of scalp EEG epochs associated with non-seizure periods and those associated with epileptic seizure events of all subjects

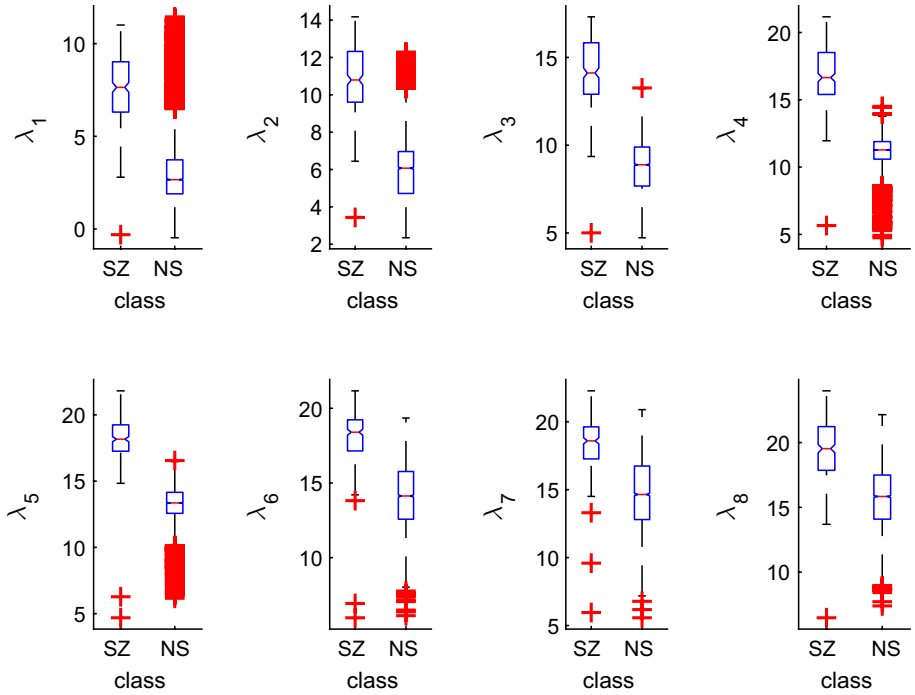

Fig. 2 Comparison between the wavelet-based features of scalp EEG epochs associated with non-seizure periods and those associated with epileptic seizure events of case chb09

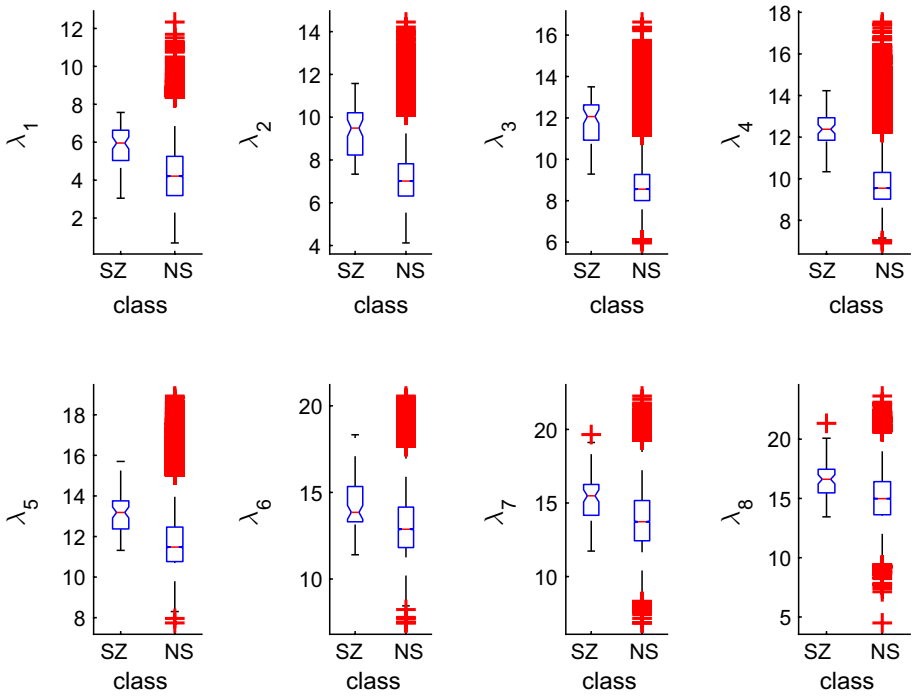

Fig. 3 Comparison between the wavelet-based features of scalp EEG epochs associated with non-seizure periods and those associated with epileptic seizure events of case chb16

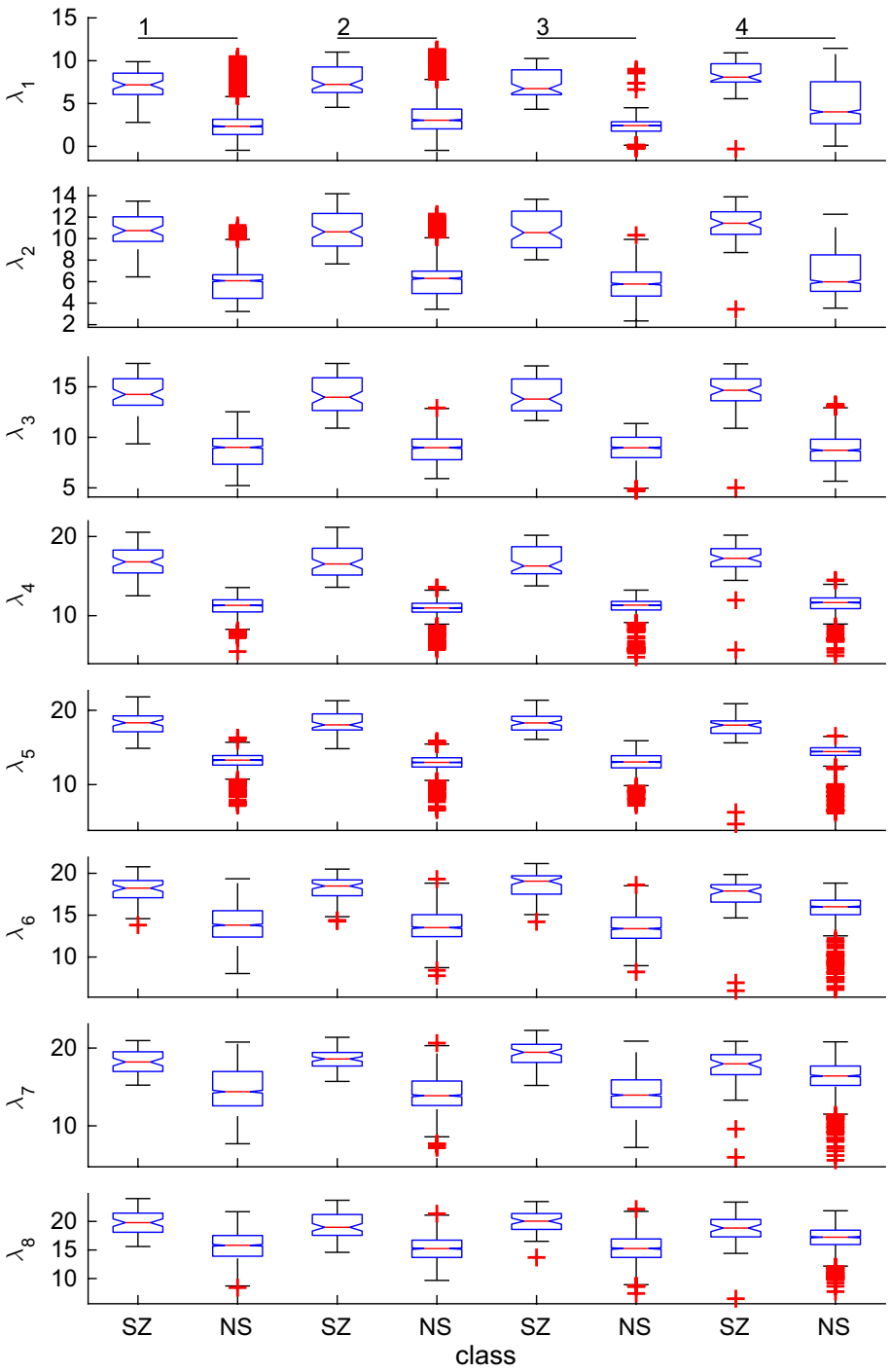

Fig. 4 Comparison of the wavelet-based features of SZ and NS epochs of case chb09 corresponding to each epileptic seizure event

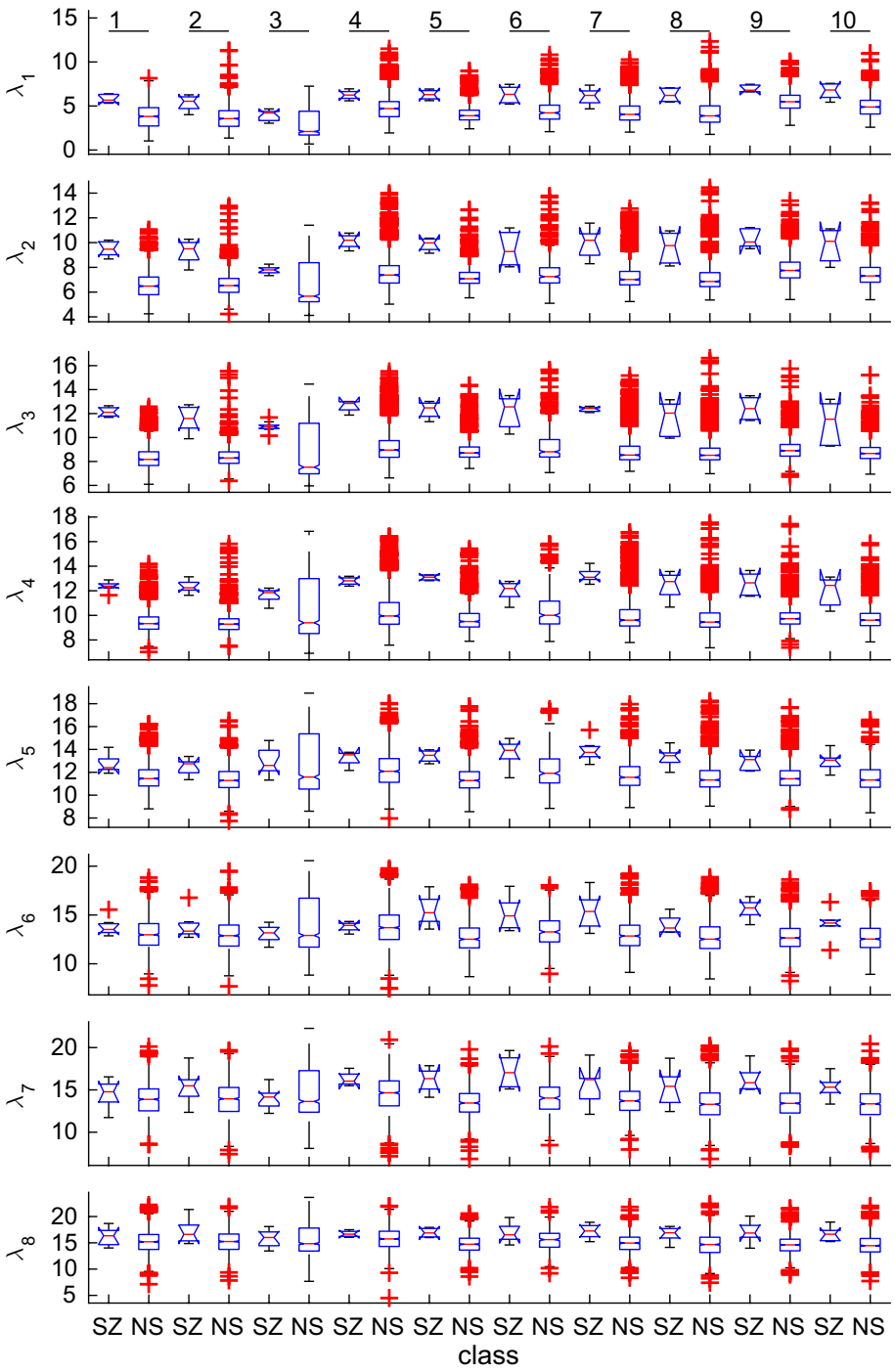

Fig. 5 Comparison of the wavelet-based features of SZ and NS epochs of case chb16 corresponding to each epileptic seizure event

5 Conclusions

The computational results suggest that the wavelet-based features obtained from the logarithm of variance of detail and approximation coefficients are a promising quantitative feature for epileptic seizure classification. Accompanied with SVM, an excellent performance on patient-dependent epileptic seizure classification can be achieved using wavelet-based features of a single channel of scalp EEG. Three key factors having an effect on the performance of epileptic seizure classification are consistency of features/patterns of epileptic seizure activity (epileptiform activity), duration of epileptic seizures, and amount of training data. In cases whose characteristics of scalp EEGs associated with epileptic seizure activity and non-seizure period are consistent, only two wavelet-based

features of a single channel of scalp EEGs are required to achieve an excellent epileptic seizure classification. The performance on epileptic seizure classification can, however, be further improved by refining relevant parameters. This will be studied in future works. Also, the epileptic seizure classification can be potentially applied for real-time (online) epileptic seizure detection and monitoring system.

Acknowledgements This work is supported by a TRF Research Career Development Grant, jointly funded by the Thailand Research Fund (TRF) and Ubon Ratchathani University, under the Contract No. RSA5880030.

References

1. Abry P, Goncalves P, Flandrin P (1993) Wavelet-based spectral analysis of $1/f$ processes. IEEE international conference on acoustics, speech, and signal processing, p. III–237–III–240
2. Andrade-Valenca LP, Dubeau F, Mari F, Zelmann R, Gotman J (2011) Interictal scalp fast oscillations as a marker of the seizure onset zone. Neurology 77:524–531
3. Goldberger AL, Amaral LAN, Glass L, Hausdorff JM, Ivanov PC, Mark RG et al (2000) PhysioBank, physiotoolkit, and physionet: components of a new research resource for complex physiologic signals. Circulation 101(23):e215–e220
4. Greene BR, Faul S, Marnane WP, Lightbody G, Korotchikova I, Boylan GB (2008) A comparison of quantitative EEG features for neonatal seizure detection. Clin Neurophysiol 119:1248–1261
5. Hopfengärtner R, Kasper BS, Graf W, Gollwitzer S, Kreiselmeyer G, Stefan H et al (2014) Automatic seizure detection in long-term scalp EEG using an adaptive thresholding technique: a validation study for clinical routine. Clin Neurophysiol 125:1346–1352
6. Janjarasjitt S (2015) Spectral exponent characteristics of intracranial EEGs for epileptic seizure classification. IRBM 36:33–39
7. Kiranyaz S, Ince T, Zabihi M, Ince D (2014) Automated patient-specific classification of long-term electroencephalography. J Biomed Inform 49:16–31
8. Klass D, Daly D (1979) Current practice of clinical electroencephalography. Raven Press, New York
9. Logesparan L, Casson AJ, Rodriguez-Villegas E (2012) Optimal features for online seizure detection. Med Biol Eng Comput 50:659–669
10. Mallat SG (1989) A theory for multiresolution signal decomposition: the wavelet representation. IEEE Trans Pattern Anal Mach Intell 11:674–693
11. Mallat S (1998) A wavelet tour of signal processing. Academic Press, San Diego
12. Meier R, Dittrich H, Schulze-Bonhage A, Aertsen A (2008) Detecting epileptic seizures in long-term human EEG: a new approach to automatic online and real-time detection and classification of polymorphic seizure patterns. J Clin Neurophysiol 25:1–13
13. National Institute of Neurological Disorders and Stroke (2016) The epilepsies and seizures: hope through research [cited April 8, 2016]. http://www.ninds.nih.gov/disorders/epilepsy/detail_epilepsy.htm#192723109
14. Paivinen N, Lammi S, Pitkanen A, Nissinen J, Penttonen M, Gronfors T (2005) Epileptic seizure detection: a nonlinear viewpoint. Comput Methods Progr Biomed 79:151–159
15. Saab ME, Gotman J (2005) A system to detect the onset of epileptic seizures in scalp EEG. Clin Neurophysiol 116:427–442
16. Shoeb AH (2009) Application of machine learning to epileptic seizure onset detection and treatment. Massachusetts Institute of Technology
17. Shoeb A, Edwards H, Connolly J, Bourgeois B, Treves S, Guttag J (2004) Patient-specific seizure onset detection. Epilepsy Behav 5:483–498
18. Temko A, Thomas E, Marnane W, Lightbody G, Boylan G (2011) EEG-based neonatal seizure detection with support vector machines. Clin Neurophysiol 122:464–473
19. Daubechies I (1992) Ten lectures on wavelets. SIAM, Philadelphia
20. Tyner FS, Knott JR, Mayer WB (1983) In: Fundamentals of EEG technology: basic concepts and methods, vol 1. Lippincott Wiliams & Wilkins
21. World Health Organization (2016) Epilepsy [cited April 8, 2016]. http://www.who.int/mediacentre/factsheets/fs999/en/
22. Wornell GW (1993) Wavelet-based representations for the $1/f$ family of fractal processes. Proc IEEE 81:1428–1450
23. Worrell G (2012) High-frequency oscillations recorded on scalp EEG. Epilepsy Curr 12:57–58

Suparerk Janjarasjitt is currently an Assistant Professor at the Department of Electrical and Electronic Engineering, Ubon Ratchathani University in Ubon Ratchathani, Thailand. His main research interest is the development of advanced computational tools and techniques for various applications spanning from engineering to biology and medicine.